INTERACTION OF CRACKS UNDER DYNAMIC LOADING

Ch. Zhang*, D. Gross*

The elastodynamic problem of straight cracks in an infinite plate which is loaded by harmonic waves is solved by an integral equation method. Furthermore, rectangular plates containing two or more cracks under impact load are investigated by the finite difference method. Numerical results for the stress intensity factors are presented.

1. INTRODUCTION

The interaction of cracks under dynamic loading has been discussed only for a few special cases up to now. Using integral transform methods Jian and Kanwal [1] and Itou [2] studied for instance two coplanar cracks in an infinite elastic plate under the action of normal incident plane harmonic waves. Impact loaded rectangular plates containing cracks have been treated in [3] by means of the finite difference method. Such problems were also investigated experimentally by Kalthoff et.al.[4]. All results show that dynamic crack interaction phenomena are quite different from static ones.

In the present paper two group of problems are considered. The first one concerns an infinite plate weakened by a set of straight cracks which are subjected by harmonic waves. This problem will be formulated in terms of integral equations which can be solved numerically. The second group are rectangular plates

* Institute of Mechanics, TH Darmstadt,
West Germany

with two or more cracks which are loaded by an impact. For this problem a computer program is developed which bases on the finite difference method.

2. INTEGRAL EQUATIONS FOR A CRACKED INFINITE PLATE

We consider the plane strain or plane stress state of an infinite plate containing N straight cracks of length $2a_k$ (k = 1,...,N). The configuration of the cracks and the notation is specified in figure 1.

Let time-harmonic elastic P or SV waves (the factor $\exp(-i\omega t)$ is ommitted throughout the analysis) impinge on the cracks. These waves cause scattered waves due to the presence of the cracks. The total displacement and stress field therefore consists of the incident field u^i_α , $\sigma^i_{\alpha\beta}$ and the scattered field u^s_α , $\sigma^s_{\alpha\beta}$:

$$u_\alpha = u^i_\alpha + u^s_\alpha \,, \qquad \sigma_{\alpha\beta} = \sigma^i_{\alpha\beta} + \sigma^s_{\alpha\beta} \,. \tag{1}$$

Both the partial fields and the total fields fulfill the equation of motion and Hookes law. Furthermore, the scattered field must satisfy the radiation conditions. Because the crack faces are traction free the boundary condition can be written as

$$\sigma_{\alpha\beta}(x^\ell_1,0)\; n^\ell_\beta = 0 \,, \qquad |x^\ell_1| \le a_\ell \,. \tag{2}$$

If the incident field is known, the main task consists in the determination of the scattered field. For this purpose we use the representation theorem for the scattered displacements [5]:

$$u^s_\gamma(\underline{x}') = \sum_{k=1}^{N} \int_{-a_k}^{a_k} \sigma^g_{\delta\varepsilon\gamma}\; n^k_\varepsilon\; \psi^k_\delta \; dx^k_1 \,. \tag{3}$$

Herein $\psi^k_\delta(x^k_1)$ denotes the displacement jump across the cracks and $\sigma^g_{\delta\varepsilon\gamma}(\underline{x}^k, \underline{x}')$ is the Greens function. From (3) and Hookes law the stresses can be derived. Using a dimensionless coordinate $t = x^k_1/a_k$ this leads together with (1) and (2) to the set of N integral equations

$$\sigma^i_{\alpha\beta}(\underline{x}^\ell)\, n^\ell_\beta = -\lim_{\underline{x}'\to\underline{x}^\ell} \sum_{k=1}^{N} a_k \int_{-1}^{1} \Big\{ \lambda \frac{\partial}{\partial x'_\gamma}\, \sigma^g_{\delta\varepsilon\gamma}\; n^\ell_\alpha + \mu\Big[\frac{\partial}{\partial x'_\beta}\, \sigma^g_{\delta\varepsilon\alpha} + \frac{\partial}{\partial x'_\alpha}\, \sigma^g_{\delta\varepsilon\beta}\Big] n^\ell_\beta \Big\} n^k_\varepsilon\; \psi^k_\delta(t)\, dt \tag{4}$$

for the unknown quantity ψ_δ^k. The left hand side of (4) describes the known tractions along the crack faces on account of the incident wave; λ and μ are the Lamé constants.

Solutions of (4) can be found numerically [5]. The stress intensity factors then follow from

$$\begin{Bmatrix} K_{Ik}^{\pm} \\ \\ K_{IIk}^{\pm} \end{Bmatrix} = \frac{\mu\sqrt{2\pi}}{1+\varkappa} \lim_{x_1^k \to \pm a_k} \frac{1}{\sqrt{a_k \mp x_1^k}} \begin{Bmatrix} \psi_2^k(x_1^k) \\ \\ \psi_1^k(x_1^k) \end{Bmatrix} \tag{5}$$

where $\varkappa = 3-4\nu$ in plane strain and $\varkappa = (3-\nu)/(1+\nu)$ in plane stress.

3. THE FINITE DIFFERENCE METHOD

The time dependent displacement and stress field in plane elastodynamics can be described by Naviers equation

$$c_1^2 \frac{\partial^2 u_\alpha}{\partial x_\beta^2} + (c_1^2 - c_2^2) \frac{\partial^2 u_\beta}{\partial x_\alpha \partial x_\beta} = \frac{\partial^2 u_\alpha}{\partial t^2} \tag{6}$$

and Hookes law. Herein $c_1^2 = (\lambda+2\mu)/\rho$ and $c_2^2 = \mu/\rho$ denote the velocities of P waves and S waves respectively. Finally, the appropriate initial and boundary conditions are required.

If the displacement field for an initial boundary value problem of a plate with stationary cracks is found, the stress intensity factors may be calculated from the well known near field solution

$$\begin{Bmatrix} u_1 - u_1^0 \\ \\ u_2 - u_2^0 \end{Bmatrix} = \frac{K_I}{2\mu}\sqrt{\frac{r}{2\pi}}\,(\varkappa - \cos\varphi) \begin{Bmatrix} \cos\frac{\varphi}{2} \\ \\ \sin\frac{\varphi}{2} \end{Bmatrix} + \frac{K_{II}}{2\mu}\sqrt{\frac{r}{2\pi}} \begin{Bmatrix} \sin\frac{\varphi}{2}\,(2+\varkappa+\cos\varphi) \\ \\ \cos\frac{\varphi}{2}\,(2-\varkappa-\cos\varphi) \end{Bmatrix}, \tag{7}$$

in which u_i^0 is the rigid body displacement.

The numerical treatment of (6) and the calculation of the K-factors was done by a computer program which is based on the finite difference sheme. Details may be found in [6], [7].

4. RESULTS AND DISCUSSION

Examples for the interaction of two straight cracks of length 2a in an infinite plate are shown in figures 2 - 5. As dynamic loading plane harmonic P waves and SV waves with amplitudes σ_0 and τ_0 respectively and the frequency ω (or wave number $k_2 = \omega/c_2$) are assumed. The propagation direction of the waves with respect to the cracks is given by the angle Θ. The dynamic K-factors are normalized by the corresponding static values

$$K_I^{stat} = \sigma_0\sqrt{\pi a} \ , \quad K_{II}^{stat} = \tau_0\sqrt{\pi a}$$

for a single crack. All computations have been carried out for plane strain and a Poissons ration $\nu = 1/3$.

Figure 2 shows K_I versus the dimensionless wave number for two collinear cracks under P-wave loading and $\Theta = 0$. In this case at the inner and outer crack tips pure mode I conditions occur ($K_{II} = 0$). Starting at the static values the K_I-factors increase with increasing wave number; then after reaching a maximum they decrease more or less monotonically. The maximum values depend on the crack distance c whereby the influence of c is stronger for the inner crack tips than for the outer crack tips. For example in the case of $c = 2{,}5a$ the static value for the inner tips is

$$K_I^{stat} = 1{,}23\ \sigma_0\sqrt{\pi a} \ .$$

The dynamic maximum value is approximately 24 percent higher. Generally the $K(k_2a)$-curves depend strongly on the angle Θ of wave incidence. For angles $\Theta \neq 0$ also K_{II} values occur. Detailed results can be found in [5].

Results for SV-wave loading ($\Theta = 0$) of collinear cracks are plotted in figure 3. Similar as for P-wave loading there is a strong dependence on the wave number and the crack distance. Remarkable in this case is the different behaviour for the inner and outer crack tips. It also shall be noted that on account of crack interaction in both cases (P and SV) higher K-values may occur for larger crack distances c than for smaller distances. This is contrary to the result for static loading.

In figures 4 and 5 the results for two wave loaded parallel cracks of equal length 2a are shown. In this case mixed mode conditions are present. Generally the interaction of the cracks gets stronger as the cracks approach each other. For small crack distance d both modes (K_I , K_{II}) can be of the same importance. Furthermore, the dynamic magnification may be higher than for collinear cracks, as one can see from the peaks in figure 4. For all cases crack ① produces higher K-maxima than crack ② .

Some examples of impact loaded cracked rectangular plates are shown in figures 6 - 9. Hereby the stress impact is assumed as a Heaviside function. Results for two different configurations of two parallel cracks are presented in figures 6 and 7. In this case K_I as well as K_{II} is present. Because of the wave reflexions at the cracks and at the boundaries the K-curves show in their details a behavior which cannot be explained simply. Remarkable is the global "periodic" shape which is connected with repeated P-wave reflexions at the loaded boundaries and the crack faces. Of interest are also the "amplitudes" of the curves. With the corresponding static values

$$K_I^{stat} = 0{,}95\ \sigma_0\sqrt{\pi a}\ , \qquad K_{II}^{stat} = 0{,}25\ \sigma_0\sqrt{\pi a}$$

one gets for the first configuration dynamic magnification factors of approximately 2,5 for K_I and 1,6 for K_{II}. For the second configuration the magnification factors are 1,9 and 2,3 for K_I and K_{II} respectively.

Figure 8 shows the K_I-curve for a plate with two edge cracks and one interior crack. In general the stress intensity factors for the edge cracks are higher than for the interior crack.

Finally a rectangular plate with two edge cracks is considered in figure 9. It shall be noted that the maximum K_I-value in the time intervall under consideration is the second peak of the curve.

REFERENCES

[1] Jian, D.L. and Kanwal, R.P., "Diffraction of elastic waves by two coplanar Griffith cracks in an infinite elastic medium", Int. J. Solids Structures, Vol.8, 1972, pp. 961-975.

[2] Itou, S., "Dynamic stress concentration around two coplanar Griffith cracks in an infinite elastic medium", J. Appl. Mech., Vol.45, 1978, pp. 803-806.

[3] Gross, D., Zhang, Ch., "Dynamische Wechselwirkung von Rissen". In: DVM Deutscher Verband für Materialprüfung e.V.; Vorträge der 17. Sitzung des Arbeitskreises Bruchvorgänge/SVMT. Basel, 12. - 13.2.1985.

[4] Kalthoff, J.F. and Winkler, S., "Fracture Behavior under Impact", Report W 10/83, Fraunhofer-Institut für Werkstoffmechanik, Freiburg 1983.

[5] Zhang, Ch.Z., "Die Anwendung von Integralgleichungsmethoden zur Lösung dynamischer Rißprobleme", submitted for publication, TH Darmstadt, 1986.

[6] Peuser, T., "Ein Beitrag zur Analyse stationärer und instationärer dynamischer Rißprobleme". Dissertation, TH Darmstadt, 1983.

[7] Zhang, Ch., Gross, D., "Experimentelle und theoretische Untersuchungen zum mechanischen Verhalten von Biegeproben bei modifizierten Schlagbedingungen und Rißkonfigurationen", DFG-Report, No.1, 1984; No.2, 1985.

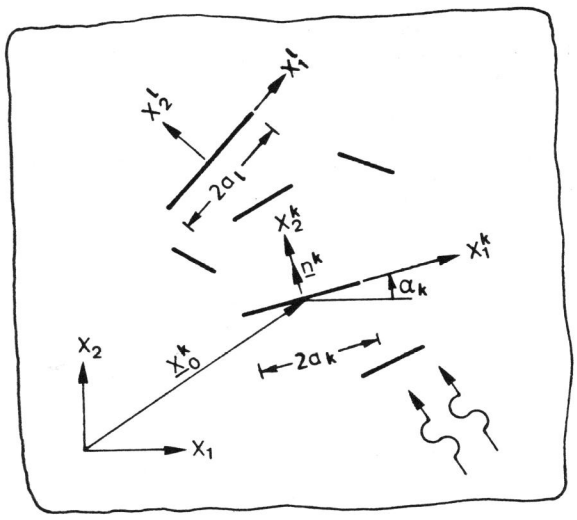

Figure 1 Infinite plate containing a set of cracks

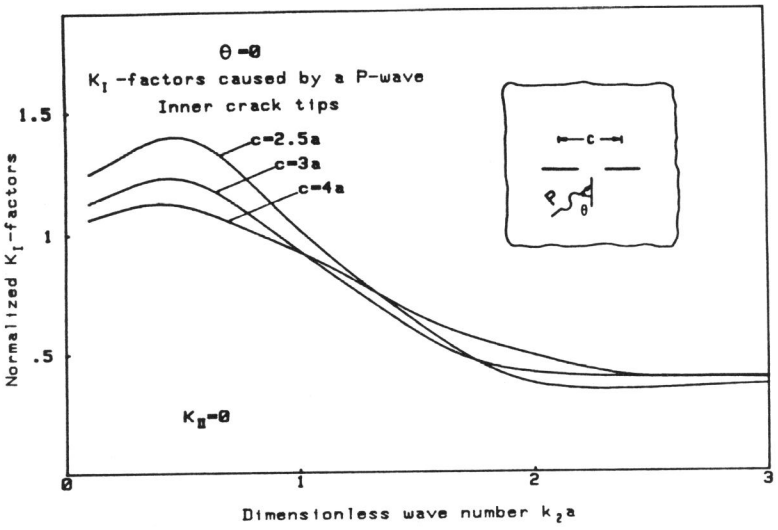

Figure 2a K_I-factors for two collinear cracks

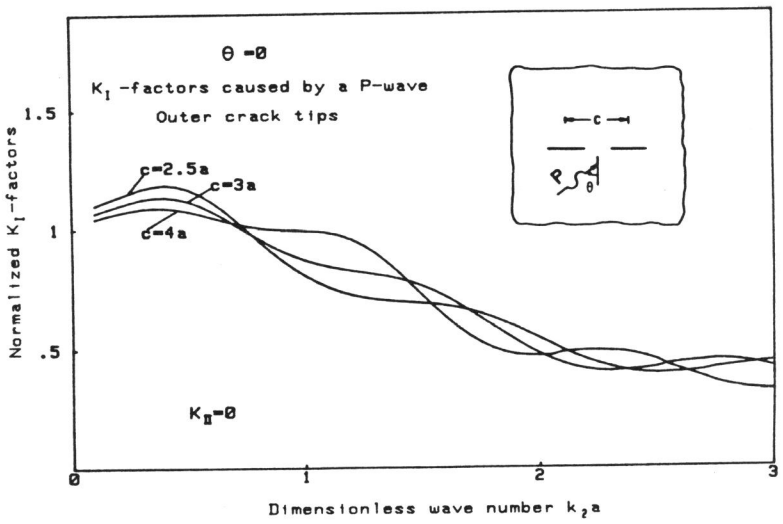

Figure 2b K_I-factors for two collinear cracks

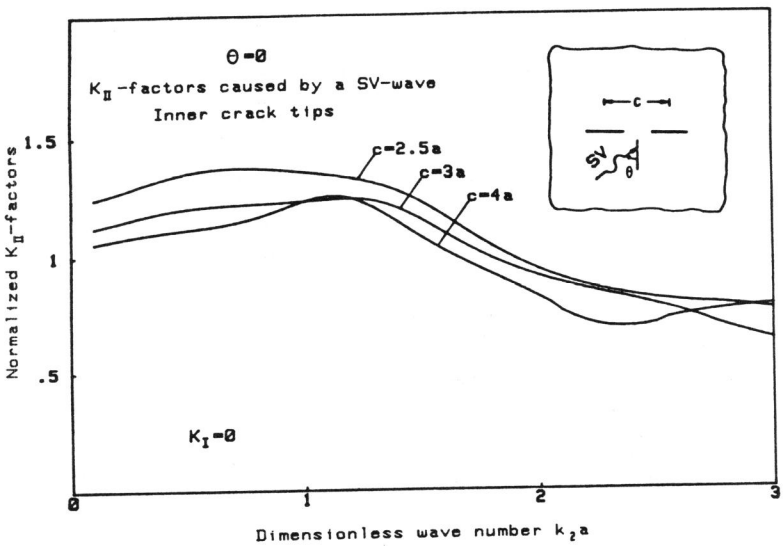

Figure 3a K_{II}-factors for two collinear cracks

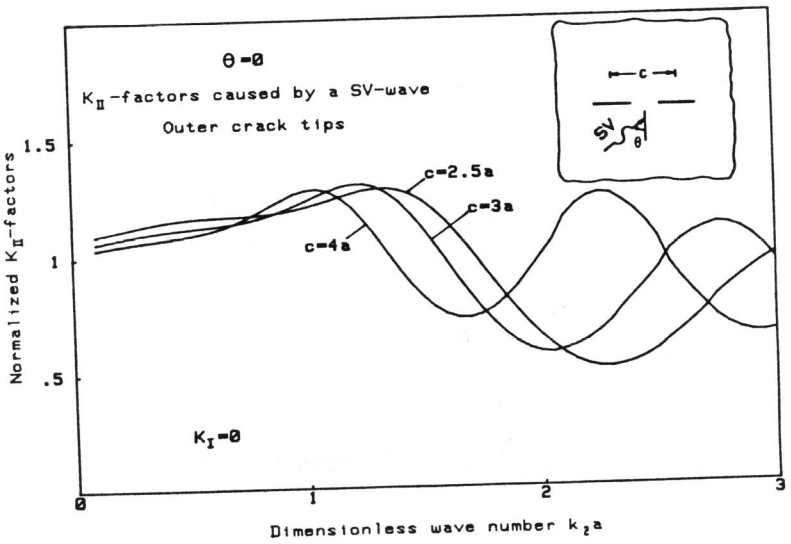

Figure 3b K_{II}-factors for two collinear cracks

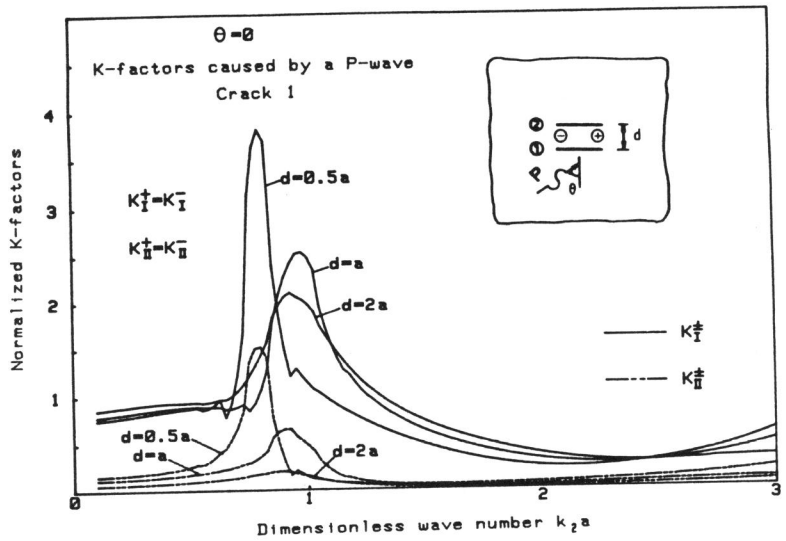

Figure 4a K-factors for two parallel cracks

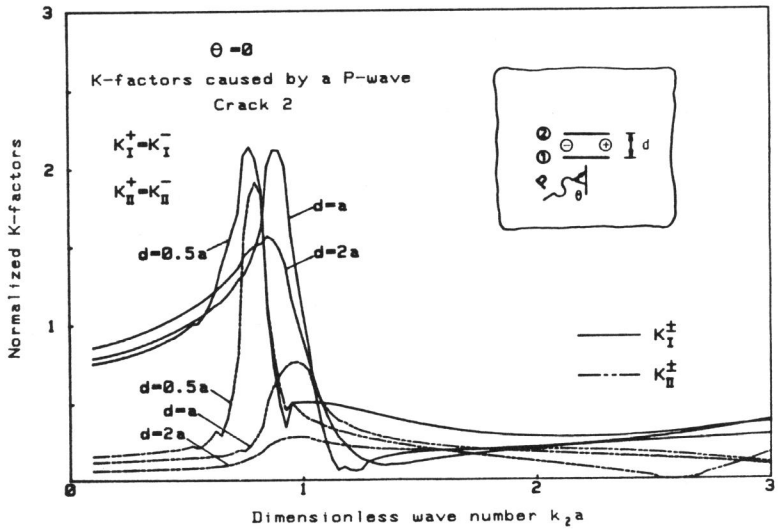

Figure 4b K-factors for two parallel cracks

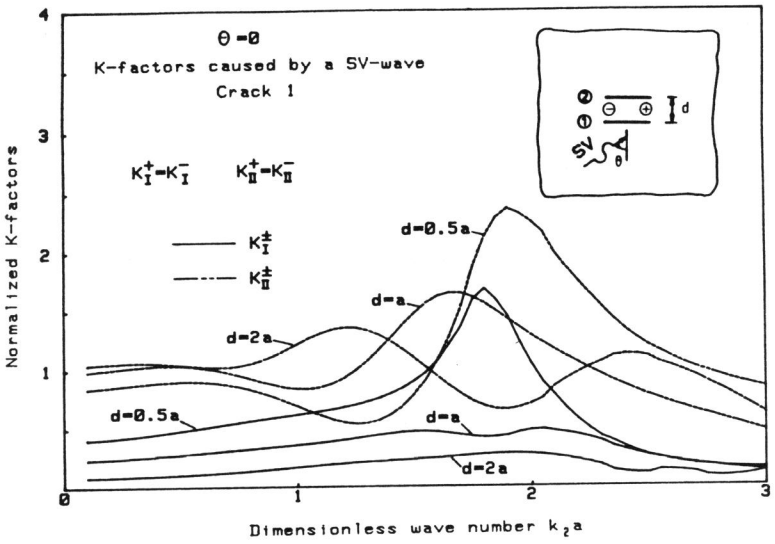

Figure 5a K-factors for two parallel cracks

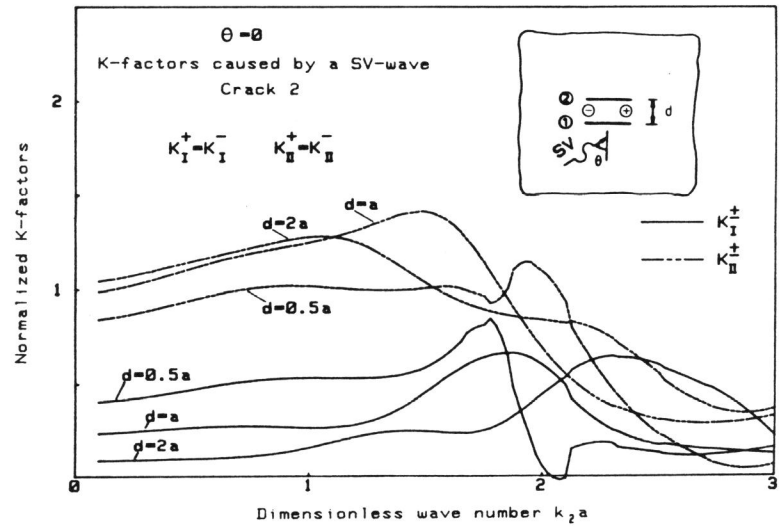

Figure 5b K-factors for two parallel cracks

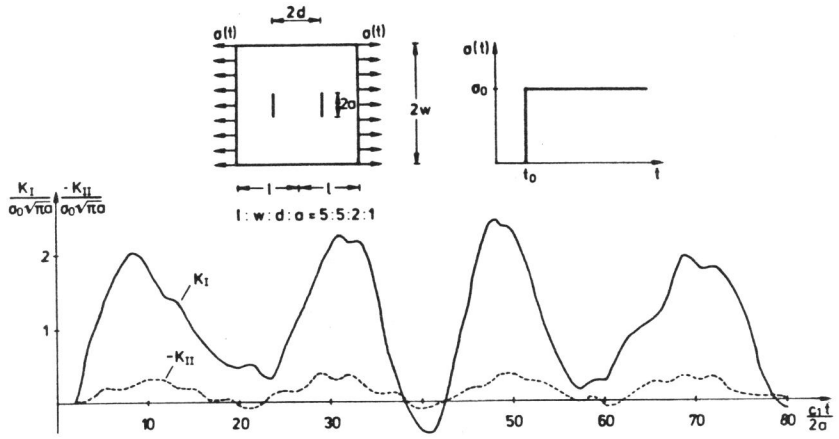

Figure 6 K-factors for a plate with two interior cracks: first configuration

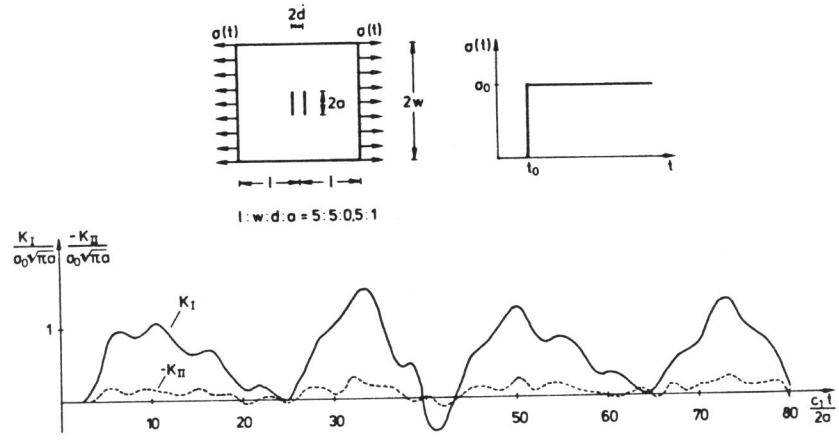

Figure 7 K-factors for a plate with two interior cracks: second configuration

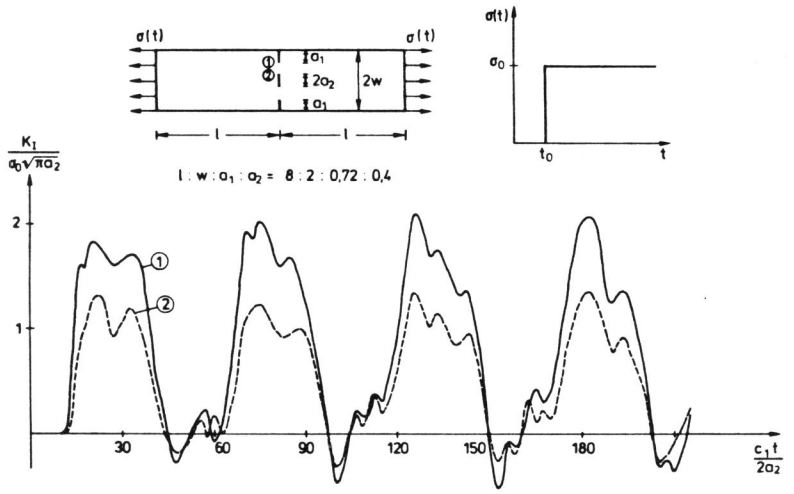

Figure 8 K-factors for a plate with two edge cracks and one interior crack

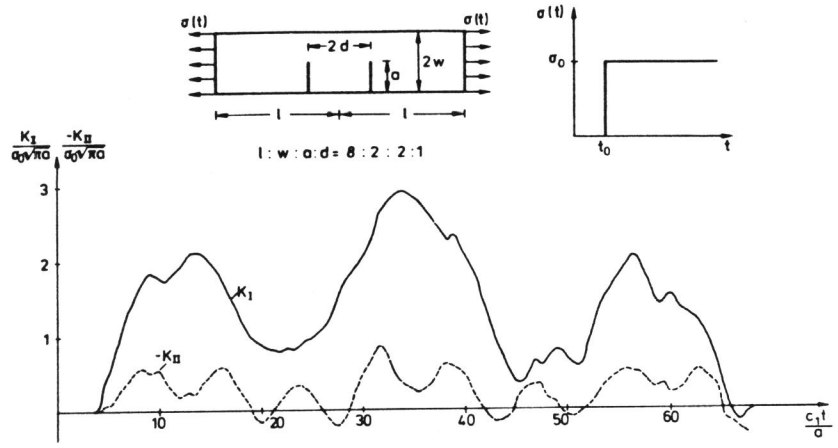

Figure 9 K-factors for a plate with two parallel edge cracks